

## Supplemental Information

### Supplemental figures titles and legends

**Figure S1, related to Figure 3.** Sample traces of action potentials and their first derivative from hippocampal CA1 pyramidal neurons in AS (**A**) and dKO (**B**) mice. The deflection point for threshold was set as the rate of rise at 30V/s. The action potential waveform is shown in blue for AS mice and in black for dKO mice, and the first derivative of the action potential is shown in green for AS mice and in red for dKO mice. The deflection point is marked by the yellow dot. (**C**) The two traces (AS mice and dKO mice) and their first derivatives are superimposed for comparison. (**D**) Sample traces of action potentials in response to injection of 10pA depolarizing current steps in current clamp. Active intrinsic properties were taken from the action potential with the closest peak to 5ms from start of injection.

**Figure S2, related to Figure 4.** (**A**) Paired-pulse facilitation PPF before and after LTP-inducing HFS in hippocampal slices from dKO mice is unchanged. n=16 slices, 8 mice. (**B**) Differences in contextual fear memory between the four genotypes are not due to alterations in memory acquisition. % freezing during acquisition was measured at the following time intervals: 1<sup>st</sup>=pre-US (2 min), 2<sup>nd</sup>=1US (1 min), 3<sup>rd</sup>=2US (1 min) and 4<sup>th</sup>=post-US (1 min). The learning acquisition curves were similar between all four genotypes. (**C**) Impaired spatial learning of the Morris water maze task by the AS mice is rescued by decreasing the expression of  $\alpha$ 1-NaKA. Escape latencies to reach the platform in the Morris water maze during the training sessions show differences between the mice. Results are the escape latencies of the 4<sup>th</sup> trial in each training session of each day. p<0.01 for genotype in 2-way-RM-ANOVA. \* denotes statistical significance p<0.05 and \*\* denotes statistical significance p<0.01 in 2-way-ANOVA for the specific time points.

**Figure S3, related to Figure 4.** Hippocampus-dependent memory deficits in AS mice are not due to sensory, motor, or emotional (anxiety) impairments, and decreasing the expression of  $\alpha$ 1-NaKA does not induce such deficits. (**A**) There are no differences in the visible Morris water maze task among the four genotypes. n=8 for WT, AS, and dKO mice; n=5 for  $\alpha$ 1-NaKA mice. (**B**) There are no differences between the four genotypes in the swim speed in the hidden platform probe trials of the Morris water maze. n=8 for WT, AS, and dKO mice; n=5 for  $\alpha$ 1-NaKA mice. (**C-E**) There are no differences between the four genotypes in the various parameters of the open field test. n=8 for WT, AS, and dKO mice; n=5 for  $\alpha$ 1-NaKA mice. These results suggest that there are no differences between the four genotypes that are related to either motor impairments (**C-D**) or anxiety (**E**). (**F**) There are no differences in the context-independent novel object recognition test. n=8 for WT, AS, and dKO mice; n=5 for  $\alpha$ 1-NaKA mice.

## Extended Experimental Procedures

**Tissue preparation and Western blots, related to Figures 1 and S4.** Mice were decapitated, the brain was quickly extracted, and hippocampi from both hemispheres were removed in an ice-cold cutting solution (CS) containing (in mM): 110 Sucrose, 60 NaCl, 3 KCl, 1.25 NaH<sub>2</sub>PO<sub>4</sub>, 28 NaHCO<sub>3</sub>, 0.5 CaCl<sub>2</sub>, 7 MgCl<sub>2</sub>, 5 glucose, and 0.6 ascorbate, and immediately snap-frozen on dry ice. Frozen hippocampi were placed in ice-cold lysis buffer containing (mM): 40 HEPES (pH=7.5), 150 NaCl, 10 pyrophosphate, 10 glycerophosphate, 1 EDTA and 0.3% CHAPS, Protease Inhibitor II, Phosphatase Inhibitor Cocktail I, II (Sigma, St. Louis, MO), and homogenized by sonication. Protein quantification was carried out with BCA (bicinchoninic acid) protein assay reagent (Thermo Scientific, Rockford, IL).

After homogenization and protein quantification, protein samples were added to  $\beta$ -mercaptoethanol-containing SDS sample buffer and heated for 2 minutes in 60°C prior to loading on SDS-polyacrylamide gels. After heating the samples, 4-20  $\mu$ g of protein (depending on the specific protein and the linear range of detection) were loaded on 4-12% gradient SDS-PAGE gels, resolved, transferred to PVDF membranes, and probed with primary antibodies using standard techniques. The primary antibodies and the dilutions for the Western blots used in these studies are as follows: NaV1.6 1:500 (Sigma-Aldrich, St. Louis, MO);  $\alpha$ 1-NaKA (clone C464.6) 1:1000 (Millipore, Billerica, MA); ankyrin-G 1:1000,  $\beta$ -actin and GAPDH 1:5000 (Santa Cruz, Santa Cruz, CA). Secondary antibodies were HRP-conjugated. All blots were developed using enhanced chemiluminescence detection (GE Healthcare, Fairfield, CT). The bands of each Western blot were imaged and quantified using the KODAK 4000MM imaging system. All signals were obtained in the linear range for each antibody, normalized by total protein, and quantified via densitometry. Data represent mean  $\pm$  s.e.m. ANOVA was used for Western blot analysis with  $p < 0.05$  as significance criteria.

**Immunostaining, related to Figure 2.** Mice were deeply anesthetized with isoflurane before transcardial perfusion with ice-cold 4% PFA in 0.1M Na-phosphate buffer (PB, pH7.2). Brains were post-fixed in 4% PFA 0.1M PB for 1 hour and equilibrated in 20% sucrose 0.1M PB over 48 hours. Afterward, 25  $\mu$ m coronal slices containing the hippocampal formation were cut on a microtome and washed in 0.1M PB. Slices were mounted on gelatin-coated coverslips, then blocked in 10% normal goat serum 0.1M PB containing 0.3% TX-100 (PBTgs). Tissue was incubated overnight at 4°C in primary antibodies diluted in PBTgs. Primary antibodies were removed by washing the tissue 3 times for 5 minutes with PBTgs. Alexa594-conjugated goat anti-mouse (1:1000) secondary antibodies diluted in PBTgs were applied for 1 hour at RT and used to visualize primary antibodies. Fluorescent dye-conjugated secondary antibodies were purchased from Invitrogen. Excess secondary antibodies were removed by consecutive 5-minute washes with PBTgs, 0.1M PB, and 0.05M PB. Fluorescence imaging was performed on an AxioImager Z1 microscope (Carl Zeiss MicroImaging) fitted with an AxioCam digital camera (Carl Zeiss MicroImaging). AxioVision acquisition software (Carl Zeiss MicroImaging) was used for collection of images. Comparison of WT and AS tissue was performed on slices prepared in parallel and images were acquired at identical exposure times. Experiments were performed at least in triplicate. Fluorescence intensity (F.I.) was measured using ImageJ (NIH). No additional processing of images was performed.

**Intracellular electrophysiology, related to Figures 3 and S1.** Brains from the four mouse genotypes were quickly removed and transverse hippocampal slices (300  $\mu$ m) were isolated with a Leica VT1200 Vibratome (Leica, Bannockburn, IL). This part of the slicing was done in ice-cold cutting solution (in mM): 110 Sucrose, 60 NaCl, 3 KCl, 1.25 NaH<sub>2</sub>PO<sub>4</sub>,

28 NaHCO<sub>3</sub>, 0.5 CaCl<sub>2</sub>, 7 MgCl<sub>2</sub>, 5 Glucose, 0.6 Ascorbate. Slices were recovered for 45 minutes at 36°C in artificial cerebrospinal fluid (ACSF) containing in mM: 125 NaCl, 2.5 KCl, 1.25 NaH<sub>2</sub>PO<sub>4</sub>, 25 NaHCO<sub>3</sub>, 25 D-glucose, 2 CaCl<sub>2</sub>, and 1 MgCl<sub>2</sub> ACSF, followed by additional recovery for 30 minutes in room-temperature ACSF. After initial recovery, slices were placed in a submerged chamber and maintained at 36°C in ACSF (2 mL/min). Slices were allowed to recover for an additional 60 minutes on the electrophysiology rig prior to experimentation. All solutions were constantly carbonygenated with 95% O<sub>2</sub> + 5% CO<sub>2</sub>. Hippocampal CA1 pyramidal cells were illuminated and visualized using a x60 water-immersion objective mounted on a fixed-stage microscope (BX51-WI, Olympus, Center Valley, PA), and the image was displayed on a video monitor using a charge-coupled device camera (Hamamatsu, Bridgewater, NJ). Recordings were amplified by multiclamp 700B and digitized by Digidata 1440 (molecular devices, Sunnyvale, CA). The recording electrode was pulled from a borosilicate glass pipette (3–5 MΩ) using an electrode puller (P-97; Sutter Instruments, Navato, CA) and filled with a K-gluconate based internal solution (in mM): 120 K-gluconate, 20 KCl, 10 HEPES, 2 MgCl<sub>2</sub>, 4 Na<sub>2</sub>ATP, 0.5 TrisGTP, 14 phosphocreatine, osmolarity 290 mOsm and PH=7.3. The recording glass pipettes were patched onto the CA1 pyramidal cells soma region. Voltages for liquid junction potential (+14mV) were not corrected online. All current-clamp recordings were low-pass filtered at 10 kHz and sampled at 50 kHz. Series resistance was compensated and only series resistance <20 MΩ was included in data set. Pipette capacitance was ~99% compensated. The method for measuring active intrinsic properties was based on previous studies that were slightly modified (Kole and Stuart, 2008). After initial assessment of the current required to induce an action potential at 15 ms from the start of the current injection with large steps (50 pA), we injected a series of brief depolarizing currents for 10 ms in steps of 10 pA increments. The first action potential that appeared on the 5ms time point was analyzed. A curve of dV/dt was created for that trace, and threshold was considered as the 30 V/s point in the rising slope of the action potential. Series resistance, input resistance, and membrane capacitance were monitored during the entire experiment. Changes of these parameters, from beginning to end of experiment, bigger than 10% were criteria for exclusion of data. Data analysis was done with Clampfit (Molecular Devices, Sunnyvale, CA). ANOVA was used for electrophysiological data analysis with p < 0.05 as significance criteria.

**Morris Water Maze (MWM), related to Figures 4 and S3:** MWM experiments were performed as previously described by our lab (Banko et al., 2005). Briefly, the paradigm consisted of 6 days of training (reference phase), where the mice were trained to locate a submerged hidden platform. , mice were given four trials per day (each trial for 60 s maximum, inter-trial interval 60 min). On the 7<sup>th</sup> day, a single-probe trial (probe test) was given after removing the hidden platform from the pool. The day after (8<sup>th</sup> day), mice were tested using a similar paradigm to find the platform by using a visible cue (visible test). The escape platform marked by a visible cue was moved randomly between four locations. The animals' trajectories, escape latencies, number of previous platform position crossing, time spent in each quadrant, and speed of the mice were recorded with a computerized video-tracking system (Noldus EthoVision).

**Open Field Test, related to Figures 4 and S3:** Open field analysis was performed as previously described (Santini et al., 2013). Briefly, mice were placed into the center of an opaque Plexiglas (44cm × 44cm × 30 cm) open-field arena in which they were allowed to explore for 30 min. The measured parameters included total distance traveled, total distance traveled in the center field of the arena, and vertical activity. The total distance was used to measure exploratory and locomotor activity. The ratio distance in the center versus periphery zone of the arena was used to assess anxiety-like behavior.

**Novel Object Recognition (NOR) test, related to Figure S3:** NOR task is based on the natural tendency of mice to explore novel rather than familiar objects. The NOR test was performed as previously described (Trinh et al., 2012). The discrimination index was calculated as the time spent exploring the novel object divided by the total time spent exploring both objects. The Noldus EthoVision software and video-tracking system were used to record the object interaction time.

### **Extended Experimental Procedures References**

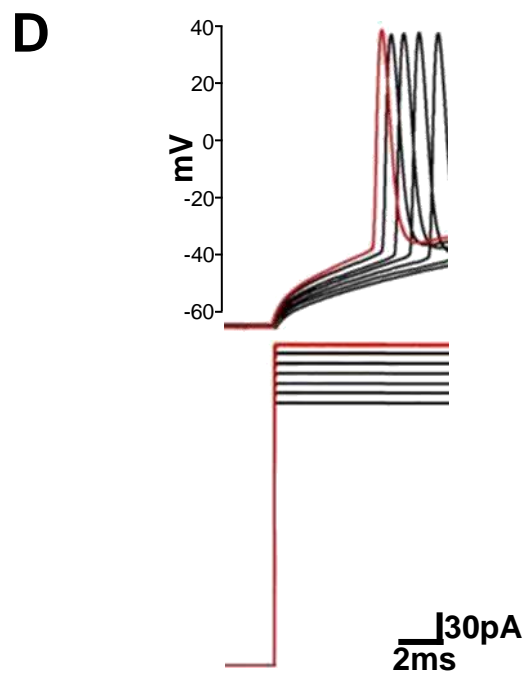
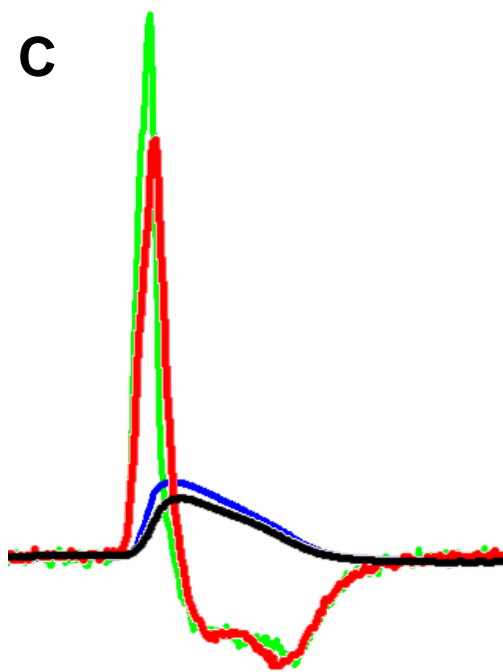
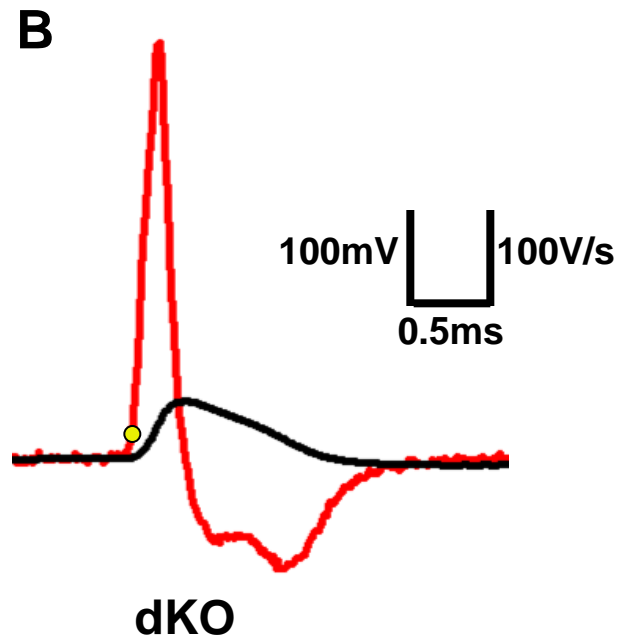
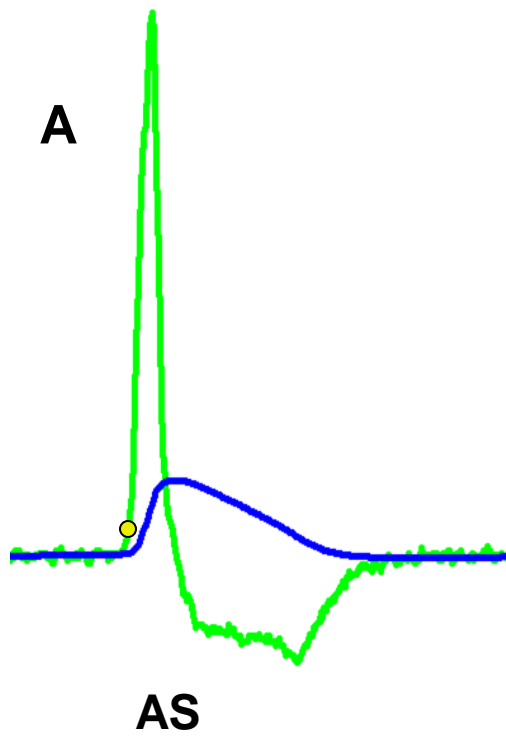
Banko, J.L., Poulin, F., Hou, L., DeMaria, C.T., Sonenberg, N., and Klann, E. (2005). The translation repressor 4E-BP2 is critical for eIF4F complex formation, synaptic plasticity, and memory in the hippocampus. *J Neurosci* 25, 9581-9590.

Kole, M.H., and Stuart, G.J. (2008). Is action potential threshold lowest in the axon? *Nat Neurosci* 11, 1253-1255.

Santini, E., Huynh, T.N., MacAskill, A.F., Carter, A.G., Pierre, P., Ruggero, D., Kaphzan, H., and Klann, E. (2013). Exaggerated translation causes synaptic and behavioural aberrations associated with autism. *Nature* 493, 411-415.

Trinh, M.A., Kaphzan, H., Wek, R.C., Pierre, P., Cavener, D.R., and Klann, E. (2012). Brain-Specific Disruption of the eIF2alpha Kinase PERK Decreases ATF4 Expression and Impairs Behavioral Flexibility. *Cell Rep* 1, 676-688.

Supplemental Figure 1



## Supp. Figure 2

